Published in final edited form as:
Biomaterials. 2010 November ; 31(31): 7971–7977. doi:10.1016/j.biomaterials.2010.07.028.

Porous nanofibrous PLLA scaffolds for vascular tissue engineering

Jiang Hu[a,1], **Xuan Sun**[b,1], **Haiyun Ma**[a], **Changqing Xie**[b], **Y. Eugene Chen**[b,2], and **Peter X. Ma**[a,c,d,2]

[a] Department of Biologic and Materials Sciences, University of Michigan Ann Arbor, MI 48109

[b] Cardiovascular Center, Department of Internal Medicine, University of Michigan Ann Arbor, MI 48109

[c] Department of Biomedical Engineering, University of Michigan Ann Arbor, MI 48109

[d] Macromolecular Science and Engineering Center, University of Michigan Ann Arbor, MI 48109

Abstract

Tissue-engineered small-diameter vascular grafts are needed for patients requiring replacement of their injured coronary and below-the-knee vessels. Understanding the interactions between the scaffolds and implanted cells and therefore the phenotype control of smooth muscle cells (SMCs) is critical for constructing functional vascular grafts. In this study, the effect of nanofibrous (NF) poly-L-lactide (PLLA) scaffolds on phenotype control of human aortic smooth muscle cells (HASMCs) was investigated. A tubular NF PLLA scaffold for blood vessel regeneration was fabricated and cell seeding studies showed cell distribution throughout the scaffold. It was found that NF PLLA scaffolds preferentially supported contractile phenotype of HASMCs under the *in vitro* culture conditions, as evidenced by elevated gene expression level of SMCs contractile markers including smooth muscle myosin heavy chain, smoothelin and myocardin. *In vivo* subcutaneous implantation studies confirmed HASMCs differentiation in the implants. Taken together, the results showed promising application of the porous NF PLLA scaffolds for reconstruction of tissue-engineered vascular grafts.

Keywords

Human aortic smooth muscle cells; Nanofibrous matrix; Porous scaffold; Differentiation; Vascular graft

Introduction

Cardiovascular diseases (CVD) are the major cause of death and disability in the Western world. In the U.S. alone, over 60 million Americans live with the effects of heart attacks or

[2]To whom correspondences should be addressed: Peter X. Ma, Ph.D., Richard H. Kingery Endowed Collegiate Professor, Department of Biologic and Materials Sciences, 1011 North University Ave., Room 2211, The University of Michigan, Ann Arbor, MI 48109-1078, Tel: (734) 764-2209, Fax: (734) 647-2110, mapx@umich.edu. Y. Eugene Chen, M.D., Ph.D., Professor, Cardiovascular Center, Department of Internal Medicine, University of Michigan Medical Center, Ann Arbor, MI 48109, Tel: (734)-936-9548, Fax: (734)-936-2641, echenum@umich.edu.
[1]Both authors contributed equally to this work

strokes, costing the U.S. approximately $350 billion per year for treatment and loss of productivity (www.americanheart.org/statistics). Vascular bypass grafting is a major treatment for ischemic heart disease and peripheral vascular disease. In the US alone, there are about 1.4 million arterial bypass operations performed annually. However, many patients who require arterial bypass procedures do not have suitable vessels for use. While large-diameter (inner diameter>6mm) blood vessels have been successfully replaced with nondegradable polymeric grafts [1], these grafts are not applicable to small-diameter (inner surface ≤6mm) blood vessels including coronary and below-the knee vessels [2]. Poor patency is largely due to thrombosis and myointimal hyperplasia. Tissue-engineered (TE) vascular grafts, resembling the natural vascular tissue structure and function, could potentially serve as an alternative source of grafts, especially for patients who lack sufficient autologous conduits [3–7]. A natural artery is typically composed of three concentric layers named the tunica intima, media and adventitia. Among these layers, the tunica media contributes significantly to the tensile strength, compliance, and vasoactive responsiveness of the blood vessels. The tunica media is composed of one or multiple layers of smooth muscle cells (SMCs) oriented approximately circumferentially, and embedded in collagen rich extra-cellular matrix (ECM), which provides the blood vessel mechanical strength and elasticity [8]. SMCs with a synthetic phenotype can rapidly proliferate and produce ECM, while a shift to a contractile phenotype with organized ECM contribute to a functional tunica media [4]. Therefore one of the key issues of constructing a functional vascular tunica media is to control the cell phenotype during the regeneration process. As the temporary artificial ECM, scaffolds play an important role in cellular differentiation as well as guiding three dimensional (3D) tissue formations [9,10]. Electrospun nanofibrous (NF) matrices have been widely used to support SMCs growth and to construct 3D tubular vascular grafts [11–15]. However, cell penetration into the scaffolds was limited due to the intrinsic small-pore feature of the electrospun NF matrices. Furthermore, the host-derived SMCs migrated onto the surface of scaffolds and caused narrowed lumen due to myointimal hyperplasia after a long term of implantation. Previously we developed a 3D scaffold with highly interconnected macro-pores and NF matrix [16] that support cell growth inside the scaffolds, and demonstrated its potential applications in constructing bone and cartilage tissues [17]. In the present study, the potential application of the porous NF scaffolds was explored for vascular tissue engineering.

Materials and methods

Fabrication of NF matrices, flat films and 3D scaffolds

Poly-L-lactide (PLLA) with an inherent viscosity of approximately 1.6 dL/g was purchased from Boehringer Ingelheim (Ingelheim, Germany). Fabrication of thin NF matrices and flat films has been previously described in details [18]. Briefly, the PLLA was dissolved in tetrahydrofuran (THF) (10% wt/v) at 60 °C and cast into a pre-heated glass mold. The mold was quickly sealed using a cover glass. The PLLA solution was phase separated at −20 °C for 2 hr and then immersed into an ice/water mixture to exchange THF for 24 hr. The matrices were washed with distilled water at room temperature for 24 hr. The obtained thin sheets of NF matrices (thickness~40μm) were then vacuum-dried for 2 days. Flat films were fabricated in a similar manner excluding the phase separation step. Instead, the solvent was evaporated at room temperature in a fume hood. The fabrication of the 3D circular NF scaffolds has been previously described in details [16]. Briefly, PLLA/THF (10% wt/v) solution was cast into an assembled sugar template (formed from bound sugar spheres, 125–250 μm in diameter) under a mild vacuum. The polymer-sugar composite was phase separated at −20 °C overnight and then immersed into cyclohexane to exchange THF for 2 days. The resulting composites were freeze-dried and the sugar spheres were leached out in distilled water and freeze-dried again to obtain highly porous scaffolds. The scaffolds were cut into circular disks with dimensions of 3.6 mm in diameter and 1 mm in thickness. For fabrication of 3D porous tubular scaffolds,

125–250 μm sugar spheres were tightly packed into a cylindrical chamber mold forming a dense porogen bed. PLLA/THF (10% wt/v) solution was poured through the porogen assembly under a mild vacuum. The polymer-sugar composite was then phase separated at −20 °C overnight and then immersed into cyclohexane to exchange THF for 2 days. The resulting composites were freeze-dried and the sugar spheres were leached out in distilled water and freeze-dried again to obtain highly porous tubular scaffolds with inner diameter of 3 mm and outer diameter of 5 mm. The tubular scaffolds were cut into 4 mm long tubes before cell seeding. For cell culture and implantation studies, the scaffolds were sterilized with ethylene oxide.

Cell culture

Adult primary human aortic smooth muscle cells (HASMCs) were obtained from Lonza (Walkersville, MD). The cells were maintained in smooth muscle growth medium-2 (Lonza) at 37°C in a humidified incubator containing 5% CO_2. NF matrices or flat films were cut into circular shapes that fit into 12-well plates and sterilized with ethylene oxide. The materials were pre-wetted by soaking in 70% ethanol for 30 min, washed three times with PBS for 30 min each, and twice in the cell culture medium for 1 hr each on an orbital shaker at 75 rpm. HASMCs were seeded at a density of 1×10^4 cells/cm^2 under static conditions. The medium was changed every two days.

The sterilized 3D scaffolds were pre-wetted by soaking in 70% ethanol for 30 min, washed three times with PBS for 30 min each, and twice in the cell culture medium for 2 hr each on an orbital shaker at 75 rpm. The medium remained in the scaffolds were carefully aspired. 0.5×10^6 cells in suspension (in 10 μl medium for circular scaffolds and in 30 μl medium for tubular scaffolds) were seeded into each scaffold drop by drop. After 2 hr of initial seeding, the cell-seeded scaffolds were further cultured in 5 mL medium for 22 hr under static condition. After that, the cell-seeded scaffolds were transferred to 6-well plates with 5 mL medium per well on an orbital shaker at 75 rpm. The medium was changed twice a week.

Scanning electron microscopy (SEM) observation

Blank scaffolds were sputter-coated with gold before SEM observation. Samples with cells were first rinsed in PBS, fixed in 2.5% glutaraldehyde and 2% paraformaldehyde overnight, and post-fixed in 1% osmium tetroxide for 1 hr. Samples were dehydrated in increasing concentrations of ethanol and hexamethyldisilizane. The samples were then sputter-coated with gold and observed under a scanning electron microscope (Philips XL30 FEG).

Gene expression analysis

Total cellular RNA from each experimental group at a pre-determined time was extracted using the RNeasy mini kit (Qiagen, Valencia, CA) according to the manufacturer's instructions and treated with DNase I (Qiagen). cDNA was synthesized with superscript III first-strand synthesis system (Invitrogen, Carlsbad, CA). Polymerase chain reaction (PCR) amplification was performed with primers for smooth muscle myosin heavy chain (SMMHC), Smoothelin and Myocardin (MyoCD) using SYBR Green supermix kit (Bio-rad, Hercules, CA) following the instructions. PCR primers and reaction conditions are described in Table 1. All RNA samples were adjusted to yield equal amplification of 18S RNA as an internal standard.

Histological analysis

Constructs were washed in PBS, fixed with 3.7% formaldehyde in PBS overnight, dehydrated through a graded series of ethanol, embedded in paraffin, and sectioned at a thickness of 5 μm. Sections were deparaffinized, rehydrated with a graded series of ethanol, and stained with H-E or Masson's trichrome method. For immunohistochemical (IHC) analysis, following

deparaffinization of sections, slides were placed in 10 mM citrate buffer for antigen unmasking. After rinsing in deionized water, quenching of endogenous peroxidase activity was achieved by incubating sections in 3% hydrogen peroxide for 10 min. After washing with deionized water and blocking with serum, tissue sections were incubated with primary antibodies to smooth muscle alpha-actin (SM-α-actin) (Millipore, Temecula, CA) or human mitochondria (Abcam, Cambridge, MA). Following a PBS rinse, sections were then incubated with biotinylated-secondary antibodies, followed by avidin-biotin complex staining (Vector labs, Burlingame, CA).

Subcutaneous implantation

After the HASMCs were seeded and cultured on scaffolds for 24 hr, the 3D circular NF scaffold-cell constructs or blank scaffolds (pre-treated in the same way as cell-containing constructs but without cell seeding) were implanted into subcutaneous pockets of nude mice. For implantation surgery, 6–8 wk old male nude mice (Charles River Laboratories, Wilmington, MA) were used. Surgery was performed under general inhalation anesthesia with isofluorane. Two midsagittal incisions were made on the dorsa and one subcutaneous pocket was created on each side of each incision using blunt dissection. One scaffold-cell construct or blank scaffold was implanted subcutaneously into each pocket at random. Four samples were implanted for each group. After placement of implants, the incisions were closed with staples. At the end of 2 wk of implantation period, the mice were euthanized and the implants were harvested. The animal procedures were performed according to the protocol approved by the University of Michigan Committee of Use and Care of Laboratory Animals.

Statistical analysis

Numerical data were reported as mean ± S.D. (n=3). To test the significance of observed differences between the study groups, the Student's *t*-test was applied. A value of $p < 0.05$ was considered to be statistically significant.

Results

Phenotype control of HASMCs on PLLA NF matrices

The HASMCs spread over a larger surface area on PLLA flat films (Fig 1A) after 24 hr of seeding and culture. In contrast, the cells showed a more rounded shape over a smaller surface area when cultured on NF matrices (Fig 1B). The expression levels of SMCs contractile phenotype-related genes were quantified. It was found that after 6 d of culture, SMMHC gene expression level was much higher for cells cultured on NF matrices compared to cells cultured on flat films (Fig 1C), while there was no significant difference in the expression levels of Smoothelin (Fig 1D) and MyoCD genes (Fig 1E).

Fabrication of 3D tubular NF scaffolds and in vitro culture of HASMCs on tubular scaffolds

A tubular NF scaffold was fabricated in a mold, combined with phase separation and porogen leaching techniques (Fig 2A). The scaffold had highly interconnected macro-pores (Fig 2B–C) and nano-scale fiber structure similar to NF matrices (Fig 2D). The HASMCs were then seeded and cultured on the 3D tubular vascular scaffolds. Histological observation with H-E staining showed that the cells were distributed throughout the scaffolds after 1 wk of *in vitro* culture (Fig 2E–F).

In vitro culture of HASMCs on 3D circular NF scaffolds

To investigate the scaffold-cell interaction, circular disk-shaped 3D NF scaffolds (3.6 mm in diameter and 1 mm in thickness) were used for HASMCs culture. The properties of the 3D circular NF scaffolds with different macro-pore sizes have been described in details in a

previous report [16]. The scaffolds consist of nanofibers with an average diameter in the order of 100 nm. Under the assembly condition of 37 °C for 15 min, the resulting scaffolds have the same high porosity of 98%, despite the differences in macro-pore size. The compressive moduli of scaffolds with different macro-pore sizes are not statistically different. In the present study, the scaffolds with macro-pore size of 125–250 μm were used in cell culture and implantation studies. The cells were seeded on scaffolds and cultured for 2 wk. After 24 hr of cell seeding, the cells aggregated inside the pores of the scaffolds (Fig 3A–B). The expression levels of contractile phenotype marker genes were enhanced for cells cultured on 3D NF scaffolds during the 2 wk of culture, compared to monolayer control culture (Fig 3C–E), with elevated expression level of SMMHC, Smoothelin and MyoCD. H-E staining showed that the cells distributed throughout the whole scaffold after 2 wk of culture (Fig 3F); however, no significant collagen deposition was observed (Fig 3G).

Subcutaneous implantation of scaffold-cell constructs

After the cells were seeded and cultured on the 3D circular NF scaffolds for 24 hr, the scaffold-cell constructs or blank scaffolds were implanted into nude mice subcutaneously. After 2 wk of implantation, the implants were collected and subjected to histological analysis. The tissue growth into the scaffolds was observed on both constructs (Fig 4A) and blank scaffolds (Fig 4B) implants. Collagen was deposited into the pores of constructs implants, shown by Masson's trichrome staining (Fig 4C). While there was no staining for IgG control (Fig 4D), positive staining of SMCs with antibody to SM-α-actin was observed in the implanted constructs (Fig 4E). HASMCs remained in the constructs after 2 wk of implantation, as shown by positive IHC staining with antibody to human mitochondria (Fig 4F).

Discussion

In the present study, a tubular NF PLLA scaffold for blood vessel regeneration was fabricated. With macro-pore design, the NF scaffold is able to support the growth and differentiation of SMCs. To construct functional TE vascular grafts, the phenotype control of SMCs is critical [4]. Synthetic phenotype SMCs are able to rapidly expand and deposit ECM, while contractile phenotype SMCs are able to contract or relax in response to vasoactive factors, leading to the blood vessel constriction or dilation. We found that PLLA NF matrices support SMCs with contractile phenotype, featured by more rounded cell shapes and higher expression of some contractile phenotype related marker genes. The 3D culture on porous NF scaffolds was then investigated. The cells distributed and grew well inside the 3D scaffolds. Compared to monolayer culture, the expression levels of contractile phenotype related marker genes, including SMMHC, Smoothelin and MyoCD were all elevated, probably due to NF matrix and 3D culture conditions. It is critical to achieve a contractile SMCs phenotype at proper development stage, since uncontrolled continued proliferation of SMCs in the implanted grafts thickens the vessel wall and narrows the vessel lumen, leading to the failure of grafts [19]. Therefore, we hypothesized that NF matrix and 3D porous scaffolds are advantageous in terms of supporting implanted SMCs with contractile phenotype to reduce the risk of narrowing vessels. However, probably due to the short time and poor environment of *in vitro* culture, there was limited ECM deposition. To investigate the *in vivo* performance of 3D NF scaffolds, the scaffold-cell constructs were subcutaneously implanted into nude mice. The results showed host tissue infiltration into the entire scaffolds. Significant collagen deposition inside the scaffolds was observed after 2 wk of implantation. However, it was not clear whether the collagen was deposited by the donor cells or the infiltrated host cells. The implanted HASMCs remained in the scaffolds after 2 wk of implantation. Positive staining of SM-α-actin showed SMCs inside the implants, which is important for maintaining vascular function. Taken together, our studies showed that the porous NF PLLA scaffolds favor a contractile phenotype of HASMCs. The PLLA scaffolds remained in the implantation sites after 2 wk of implantation.

The *in vivo* degradation of NF scaffolds was not investigated in this study. However, it has been demonstrated that the high surface area of NF matrices greatly accelerated the degradation rate making them more suitable for tissue engineering applications [20]. Besides matrix effect, growth factors can greatly affect the cell proliferation and differentiation. Phenotype of SMCs has been demonstrated to be influenced by multiple growth factors, including platelet derived growth factor BB [21], transforming growth factor-β1 [22] and basic fibroblast growth factor [23]. The incorporation of a controlled-release system into the porous NF scaffolds has been achieved in our lab, without altering the porous architecture and mechanical properties of the scaffolds [24]. The controlled release of appropriated growth factors may allow us to more precisely tailor the phenotypes of SMCs along different development stages to engineer functional vascular grafts.

Conclusions

A tubular NF PLLA scaffold for blood vessel regeneration was fabricated and the cell seeding studies showed cell distribution throughout the scaffold. The *in vitro* culture studies showed that NF PLLA scaffolds preferentially supported contractile phenotype of HASMCs and *in vivo* subcutaneous implantation studies showed host tissue infiltration and HASMCs differentiation in the implants. The results have demonstrated promising application of the porous NF PLLA scaffolds for the reconstruction of tissue-engineered vascular grafts.

Acknowledgments

This work is partially funded by an Inaugural Grant (Y.E.C. and P.X.M.) from the Cardiovascular Center at University Michigan and National Institutes of Health (DE015384 and DE017689: P.X.M; HL092421 and HL068878: Y.E.C.). C.X. is supported by AHA National Scientific Development Grant (09SDG2260023). Y.E.C. is an AHA established investigator (0840025N). P.X.M. is partially supported by the Richard H. Kingery Endowed Collegiate Professorship.

References

1. Kannan RY, Salacinski HJ, Butler PE, Hamilton G, Seifalian AM. Current status of prosthetic bypass grafts: a review. J Biomed Mater Res B Appl Biomater 2005;74(1):570–581. [PubMed: 15889440]
2. Nerem RM, Seliktar D. Vascular tissue engineering. Annu Rev Biomed Eng 2001;3:225–243. [PubMed: 11447063]
3. Weinberg CB, Bell E. A blood vessel model constructed from collagen and cultured vascular cells. Science 1986;231(4736):397–400. [PubMed: 2934816]
4. Seliktar D, Black RA, Vito RP, Nerem RM. Dynamic mechanical conditioning of collagen-gel blood vessel constructs induces remodeling in vitro. Ann Biomed Eng 2000;28(4):351–362. [PubMed: 10870892]
5. Niklason LE, Gao J, Abbott WM, Hirschi KK, Houser S, Marini R, et al. Functional arteries grown in vitro. Science 1999;284(5413):489–493. [PubMed: 10205057]
6. L'Heureux N, Paquet S, Labbe R, Germain L, Auger FA. A completely biological tissue-engineered human blood vessel. FASEB J 1998;12(1):47–56. [PubMed: 9438410]
7. L'Heureux N, Dusserre N, Konig G, Victor B, Keire P, Wight TN, et al. Human tissue-engineered blood vessels for adult arterial revascularization. Nat Med 2006;12(3):361–365. [PubMed: 16491087]
8. Bank AJ, Wang H, Holte JE, Mullen K, Shammas R, Kubo SH. Contribution of collagen, elastin, and smooth muscle to in vivo human brachial artery wall stress and elastic modulus. Circulation 1996;94 (12):3263–3270. [PubMed: 8989139]
9. Ma PX. Biomimetic materials for tissue engineering. Adv Drug Deliv Rev 2008;60(2):184–198. [PubMed: 18045729]
10. Shinoka T, Shum-Tim D, Ma PX, Tanel RE, Isogai N, Langer R, et al. Creation of viable pulmonary artery autografts through tissue engineering. J Thorac Cardiovasc Surg 1998;115(3):536–545. [PubMed: 9535439]

11. Xu CY, Inai R, Kotaki M, Ramakrishna S. Aligned biodegradable nanofibrous structure: a potential scaffold for blood vessel engineering. Biomaterials 2004;25(5):877–886. [PubMed: 14609676]
12. Hashi CK, Zhu Y, Yang GY, Young WL, Hsiao BS, Wang K, et al. Antithrombogenic property of bone marrow mesenchymal stem cells in nanofibrous vascular grafts. Proc Natl Acad Sci U S A 2007;104(29):11915–11920. [PubMed: 17615237]
13. Zhang X, Wang X, Keshav V, Johanas JT, Leisk GG, Kaplan DL. Dynamic culture conditions to generate silk-based tissue-engineered vascular grafts. Biomaterials 2009;30(19):3213–3223. [PubMed: 19232717]
14. Tillman BW, Yazdani SK, Lee SJ, Geary RL, Atala A, Yoo JJ. The in vivo stability of electrospun polycaprolactone-collagen scaffolds in vascular reconstruction. Biomaterials 2009;30(4):583–588. [PubMed: 18990437]
15. He W, Ma Z, Teo WE, Dong YX, Robless PA, Lim TC, et al. Tubular nanofiber scaffolds for tissue engineered small-diameter vascular grafts. J Biomed Mater Res A 2009;90(1):205–216. [PubMed: 18491396]
16. Wei G, Ma PX. Macroporous and nanofibrous polymer scaffolds and polymer/bone-like apatite composite scaffolds generated by sugar spheres. J Biomed Mater Res A 2006;78(2):306–315. [PubMed: 16637043]
17. Hu J, Feng K, Liu X, Ma PX. Chondrogenic and osteogenic differentiations of human bone marrow-derived mesenchymal stem cells on a nanofibrous scaffold with designed pore network. Biomaterials 2009;30(28):5061–5067. [PubMed: 19564041]
18. Hu J, Liu X, Ma PX. Induction of osteoblast differentiation phenotype on poly(L-lactic acid) nanofibrous matrix. Biomaterials 2008;29(28):3815–3821. [PubMed: 18617260]
19. Sarjeant JM, Rabinovitch M. Understanding and treating vein graft atherosclerosis. Cardiovasc Pathol 2002;11(5):263–271. [PubMed: 12361836]
20. Chen VJ, Ma PX. The effect of surface area on the degradation rate of nano-fibrous poly(L-lactic acid) foams. Biomaterials 2006;27(20):3708–3715. [PubMed: 16519935]
21. Corjay MH, Thompson MM, Lynch KR, Owens GK. Differential effect of platelet-derived growth factor-versus serum-induced growth on smooth muscle alpha-actin and nonmuscle beta-actin mRNA expression in cultured rat aortic smooth muscle cells. J Biol Chem 1989;264(18):10501–10506. [PubMed: 2732233]
22. Hishikawa K, Nakaki T, Fujii T. Transforming growth factor-beta(1) induces apoptosis via connective tissue growth factor in human aortic smooth muscle cells. Eur J Pharmacol 1999;385(2–3):287–290. [PubMed: 10607888]
23. Srivastava S, Terjung RL, Yang HT. Basic fibroblast growth factor increases collateral blood flow in spontaneously hypertensive rats. Am J Physiol Heart Circ Physiol 2003;285(3):H1190–1197. [PubMed: 12763749]
24. Wei G, Jin Q, Giannobile WV, Ma PX. Nano-fibrous scaffold for controlled delivery of recombinant human PDGF-BB. J Control Release 2006;112(1):103–110. [PubMed: 16516328]

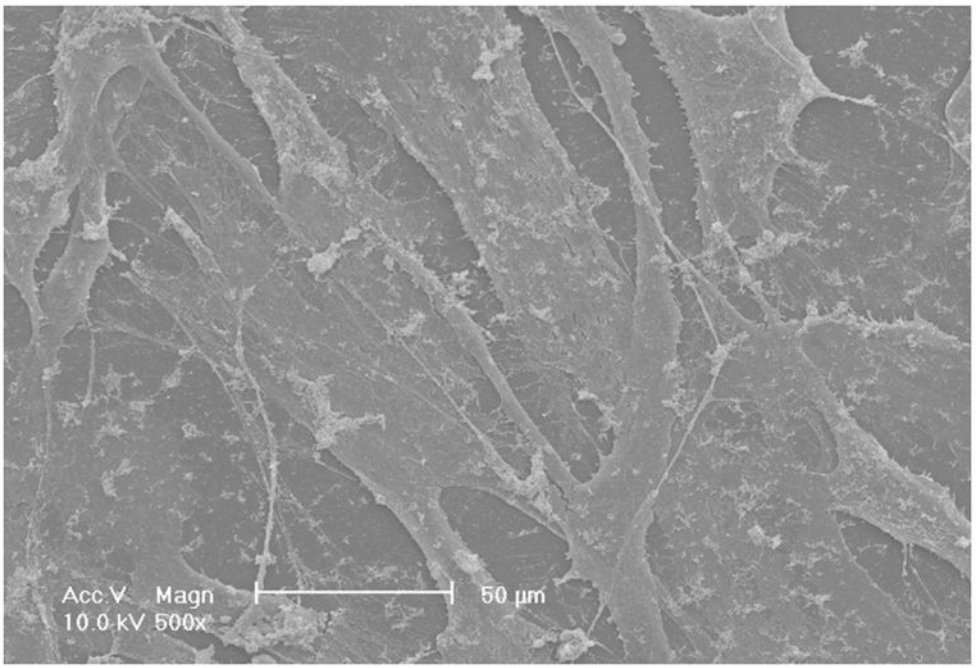

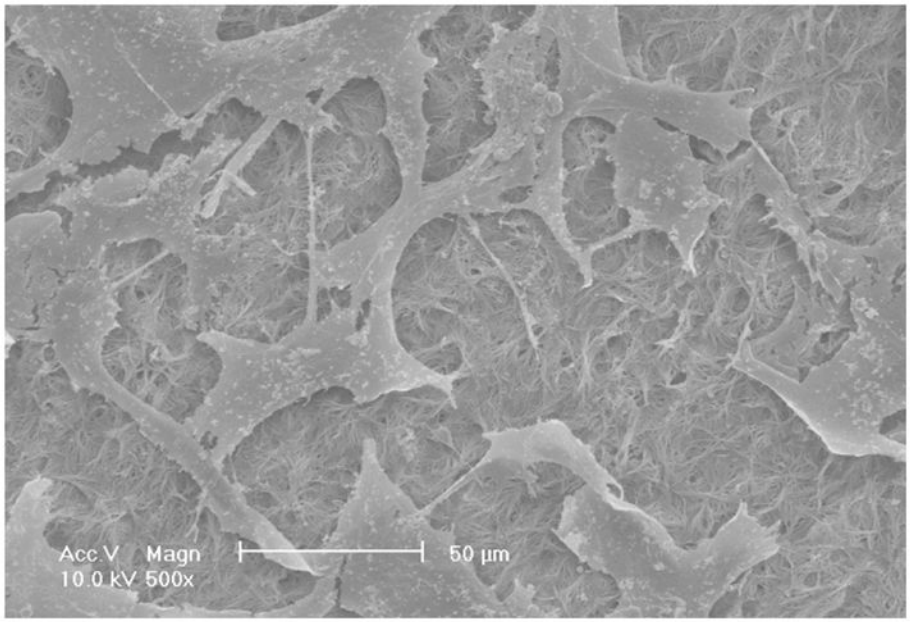

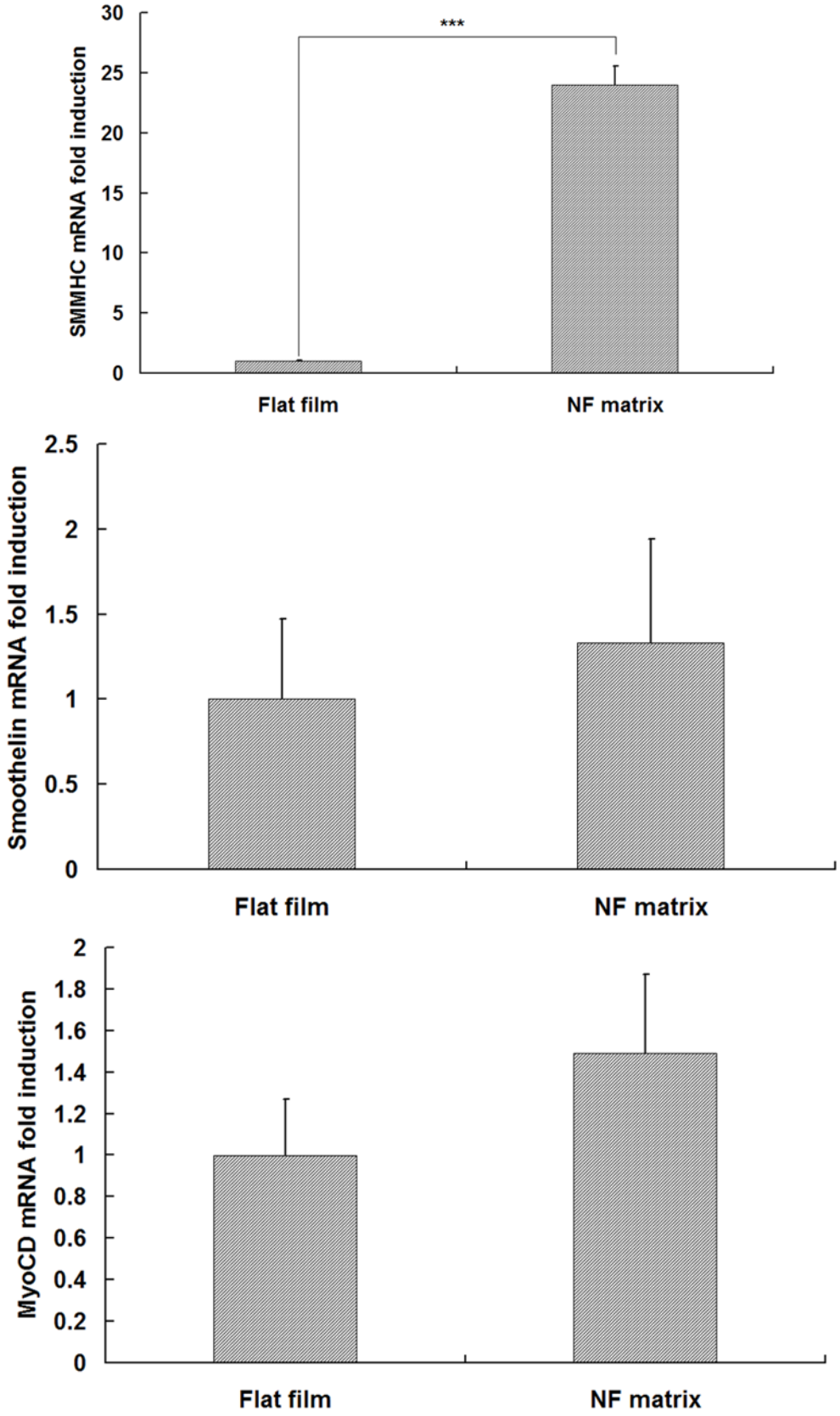

Fig. 1.

SEM micrographs of HASMCs cultured on PLLA flat films (A) and NF matrices (B) after 24 hr of seeding and culture. The cells on NF matrices were more rounded compared to cells cultured on flat films. Gene expression of SMC specific markers was analyzed on flat films or NF matrices after 6 d of culture (C–E). ***$P<0.001$.

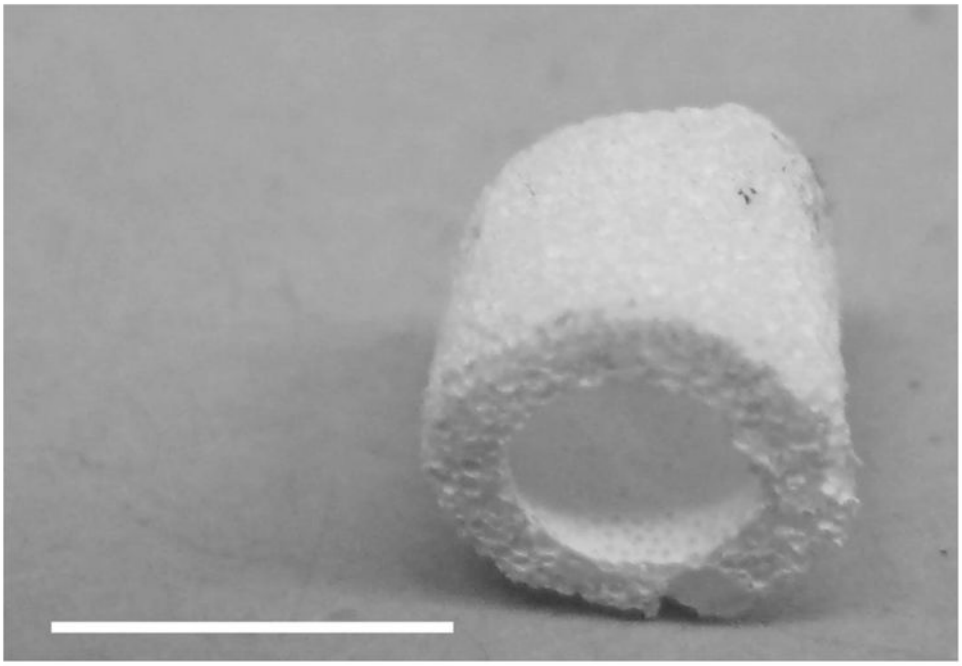

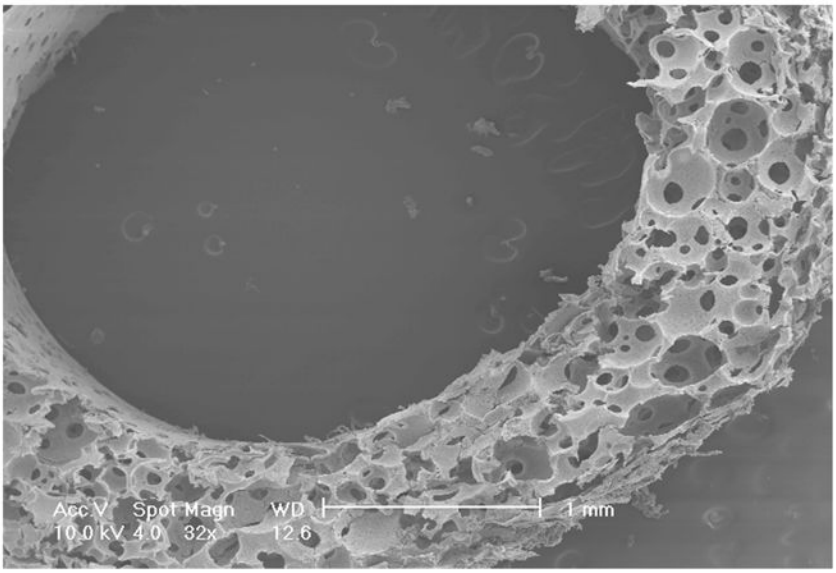

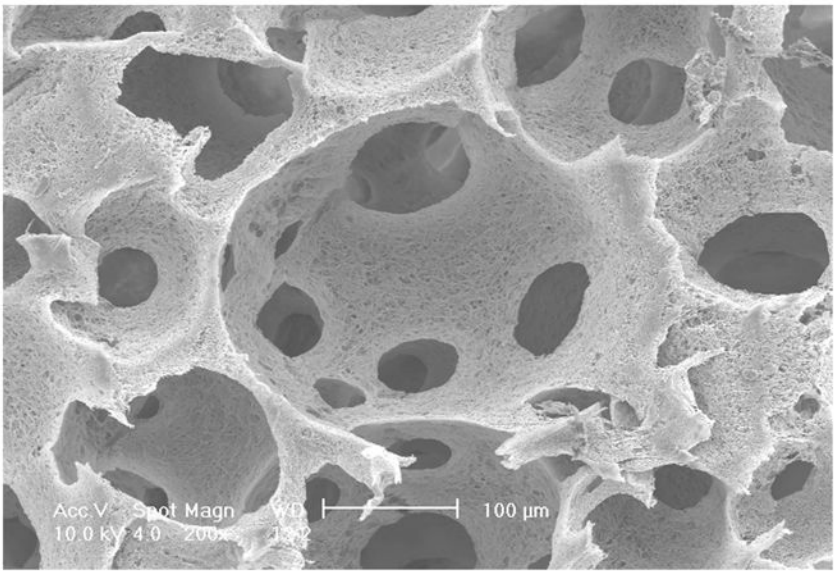

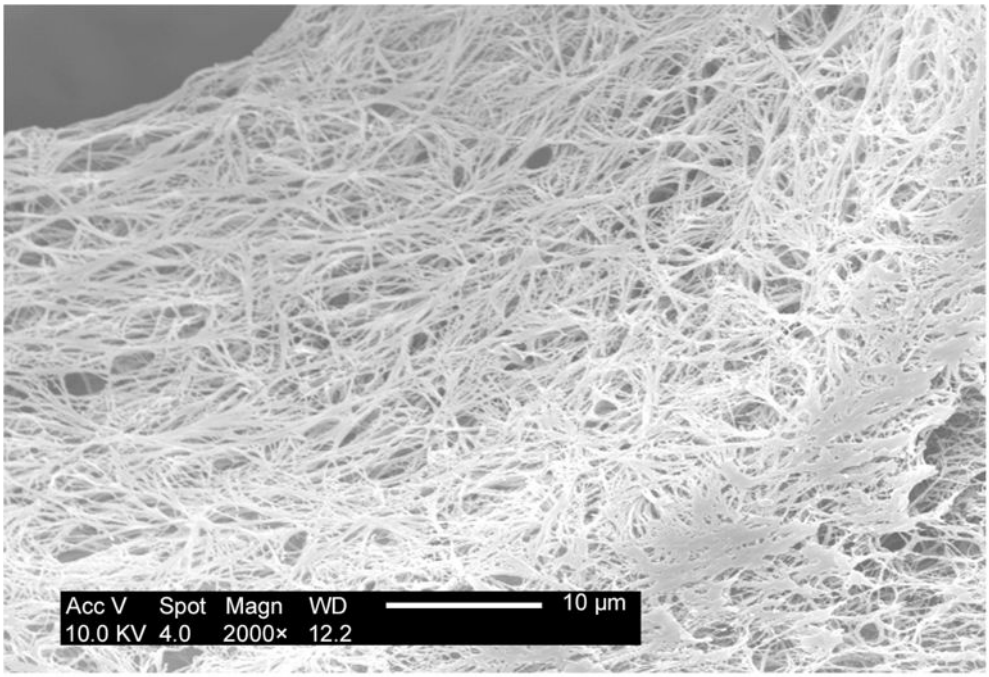

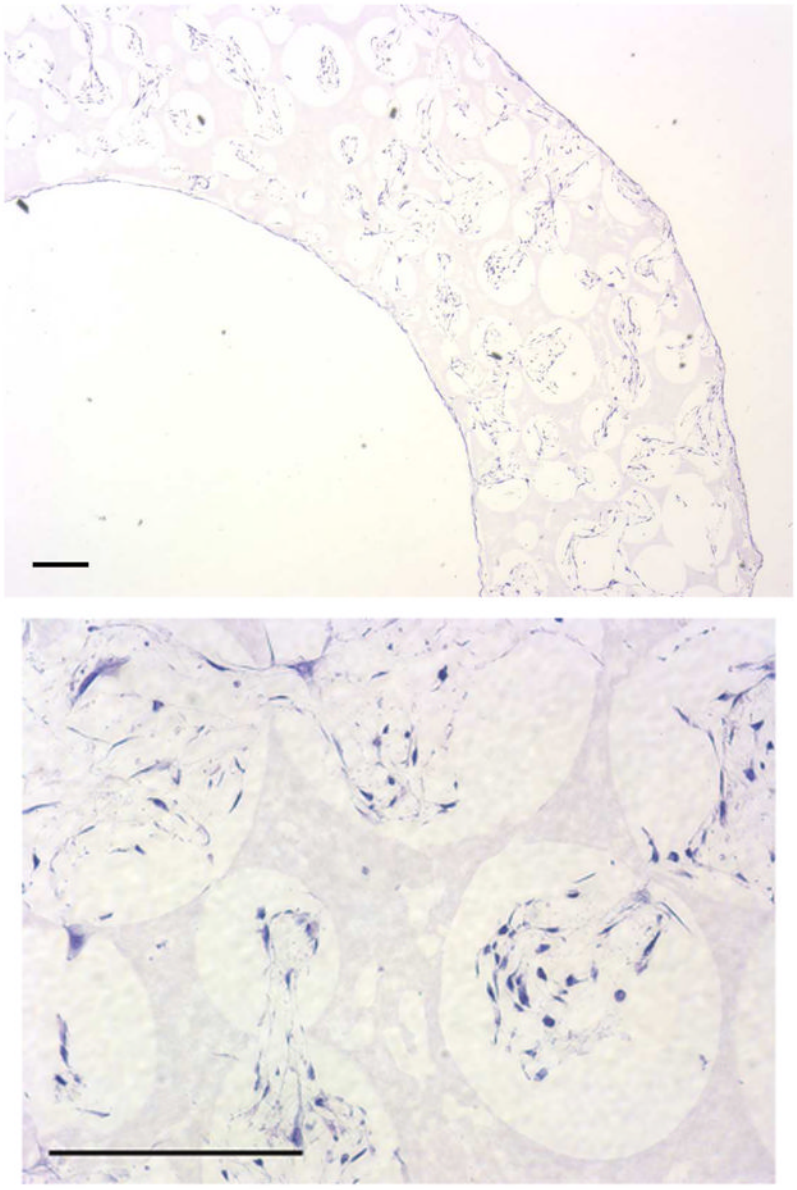

Fig. 2.

Fabrication of tubular NF scaffolds and *in vitro* cell culture on the scaffolds. Gross view of the tubular scaffold (A). Scale bar: 5mm. SEM micrographs of cross-sectioned scaffold showing gross structures (B), macro-pores, pore interconnections (C), and NF structure (D). Histological analysis of *in vitro* cultured constructs for 1 wk, stained with H-E and observed at low (E) and high (F) magnifications. Scale bar: 200μm.

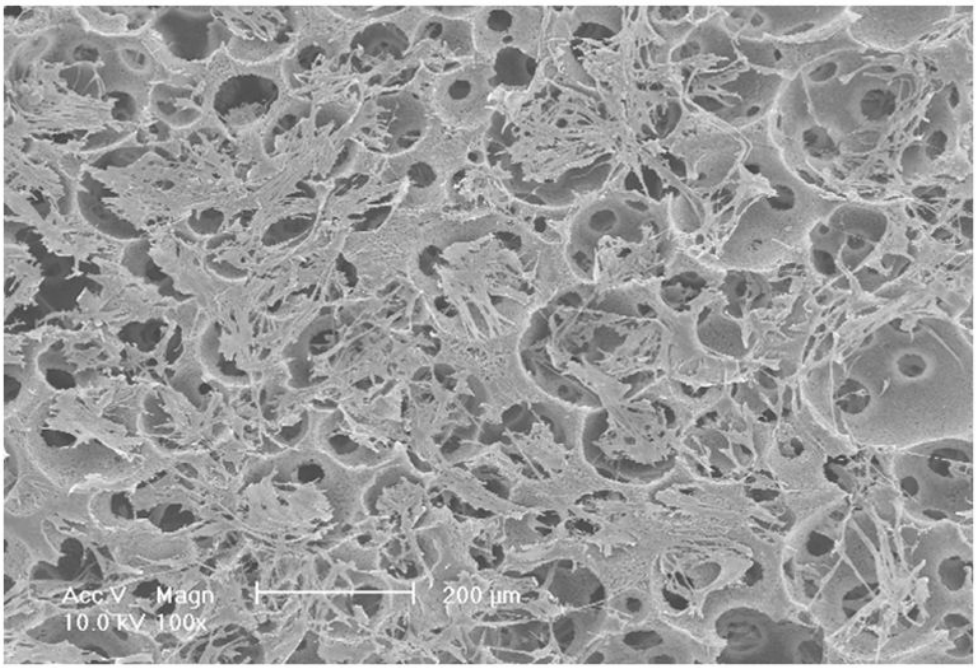

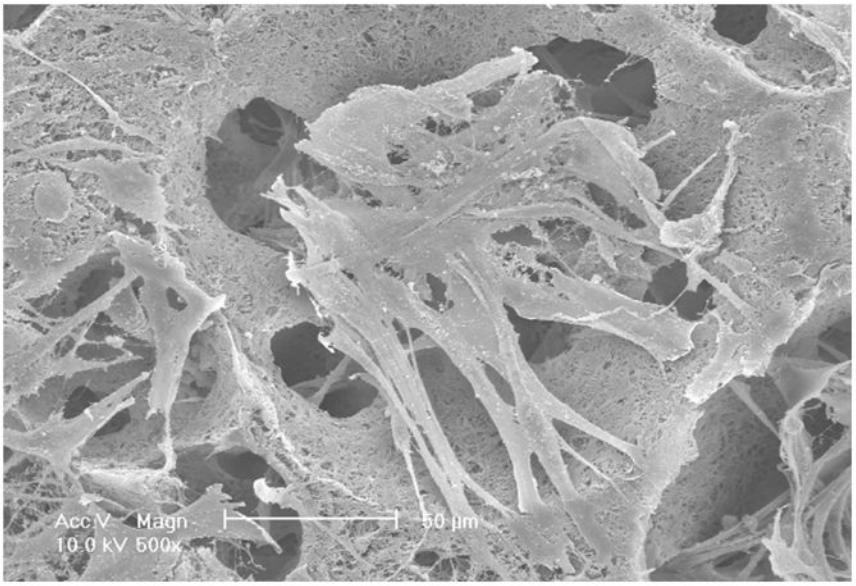

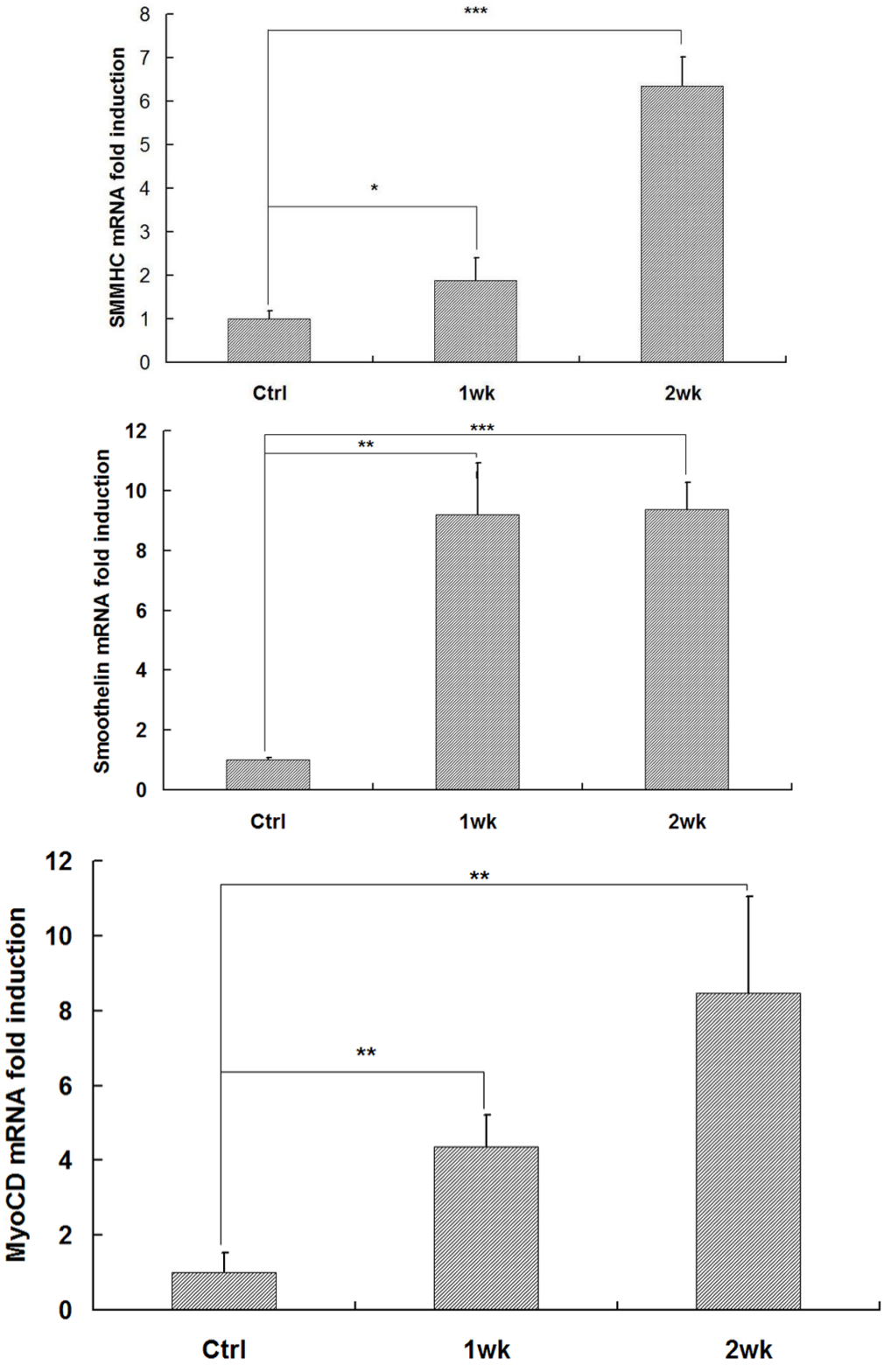

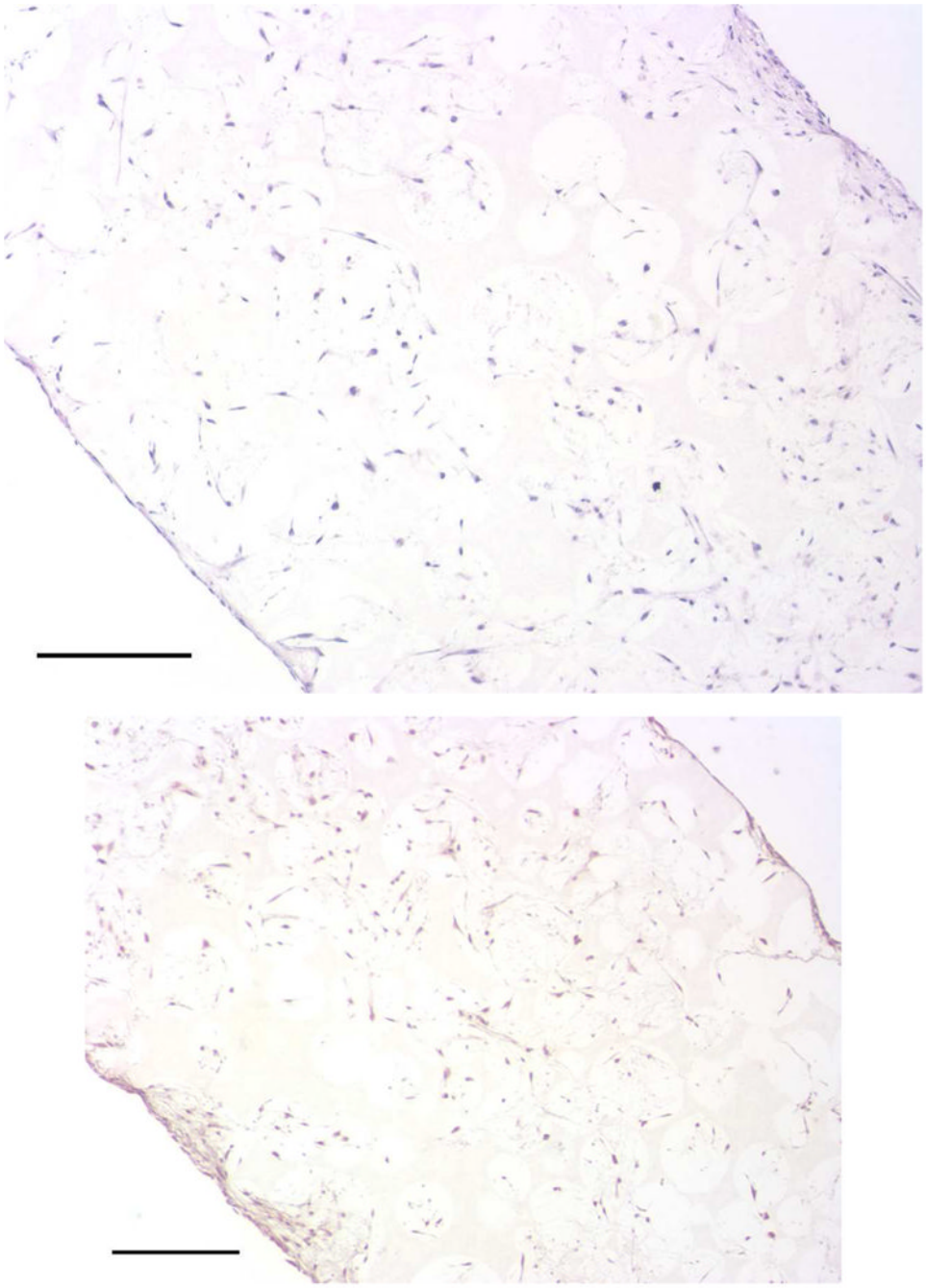

Fig. 3.

In vitro culture of HASMCs on a 3D NF scaffold. SEM micrographs of the cell-scaffold construct after 24 hr of cell seeding and culture (A, B). Gene expression of SMC specific markers was analyzed after 1 wk and 2 wk of culture on scaffolds, compared to monolayer control culture (C–E). H-E staining (F) and Masson's trichrome staining (G) of sections of constructs cultured for 2 wk. Scale bar: 200μm. * $P<0.05$, ** $P<0.01$, *** $P<0.001$.

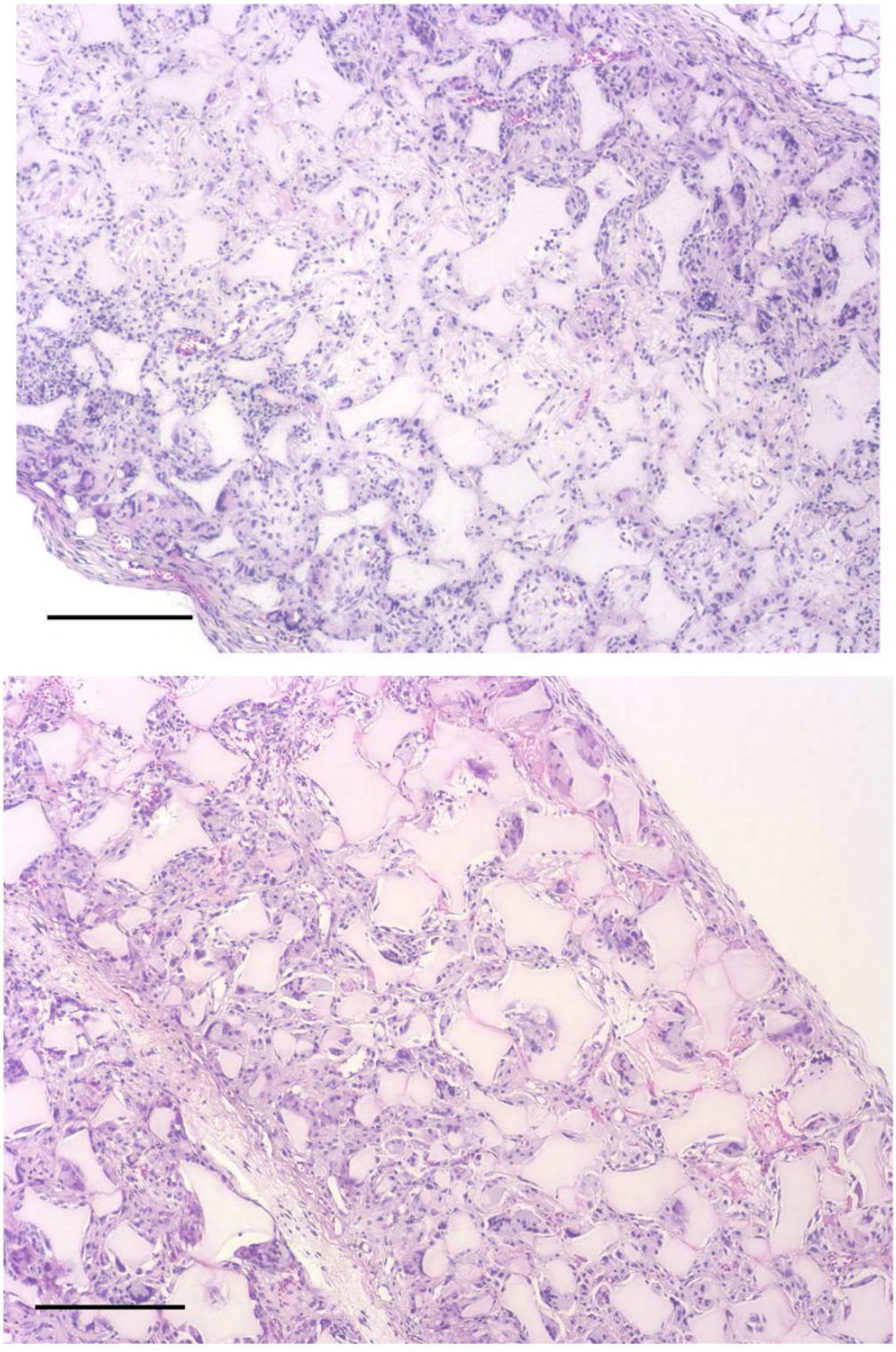

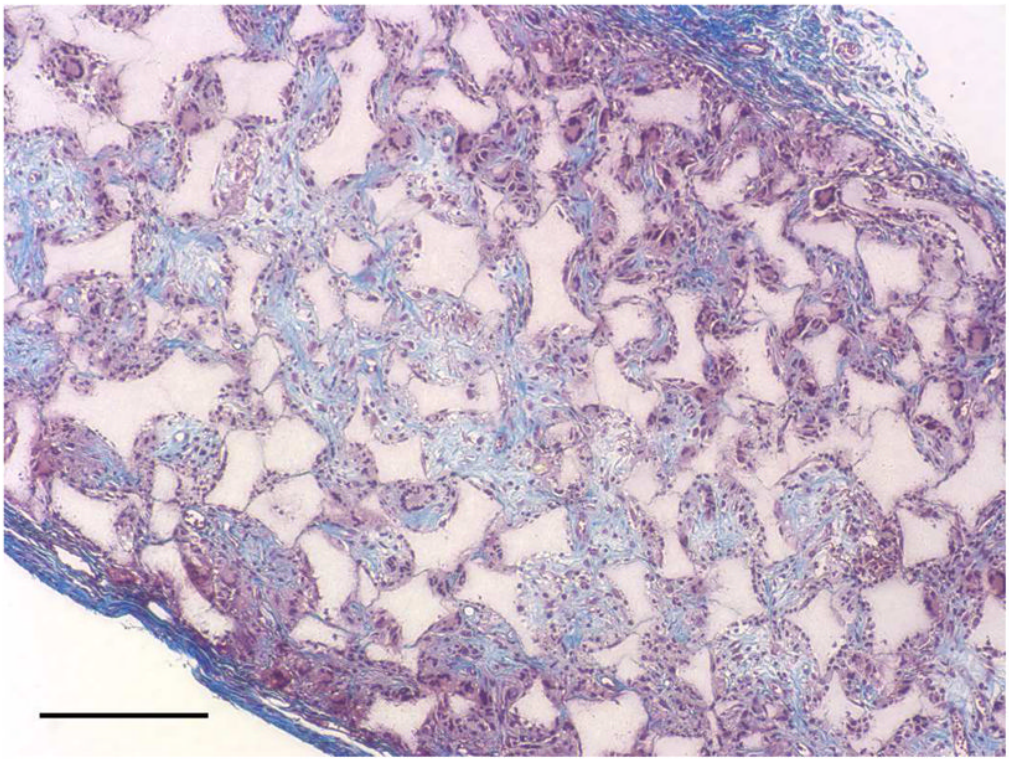

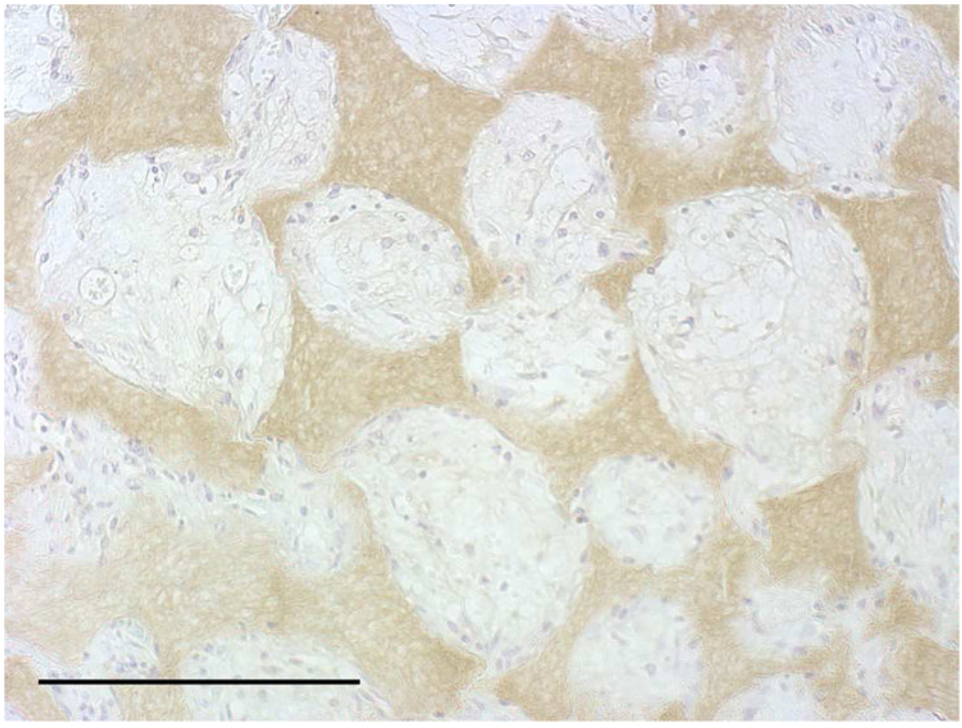

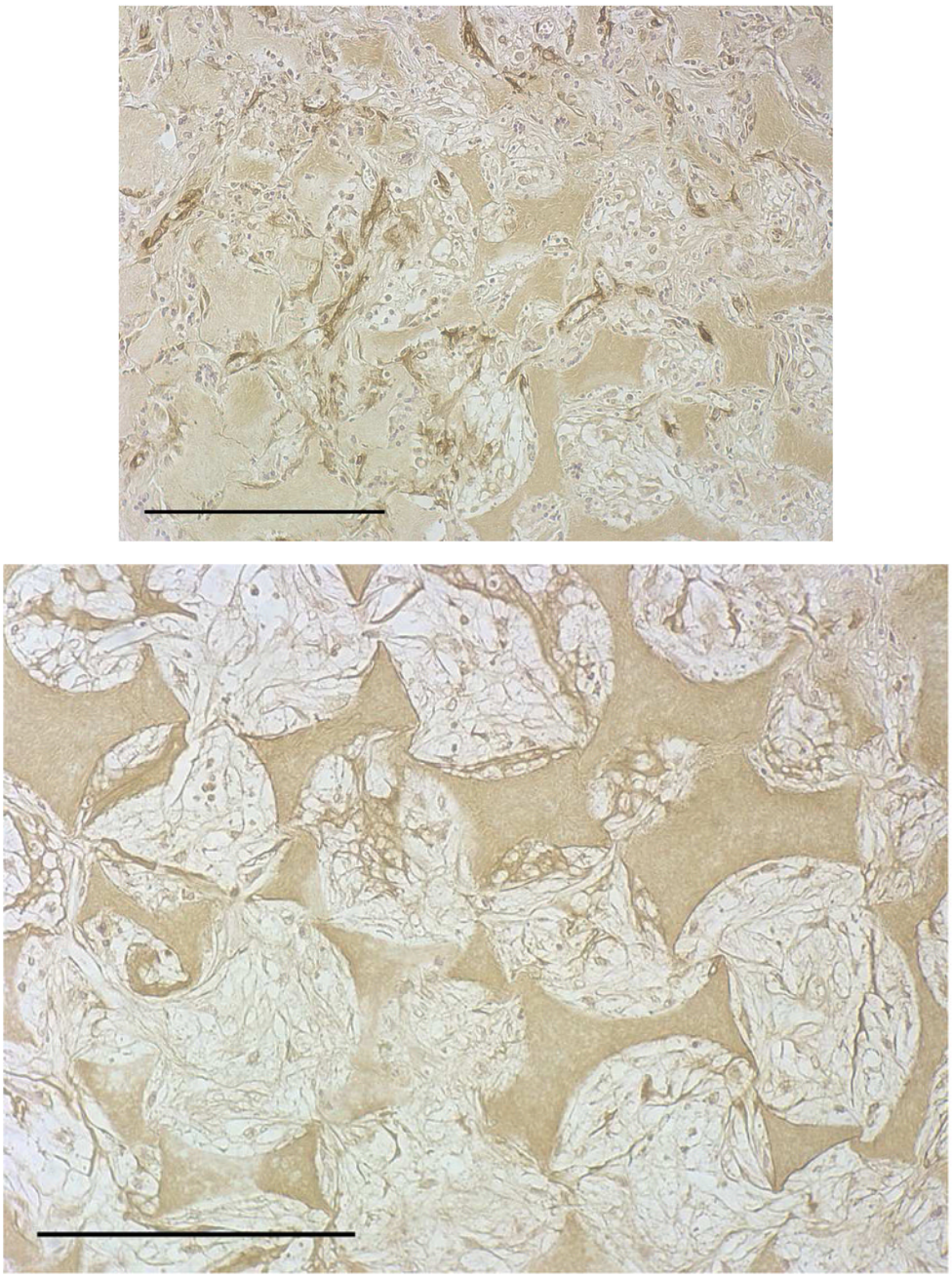

Fig. 4.

In vivo implantation of HASMCs-scaffold constructs after 24 hr of cell seeding and culture: H-E staining of sections of constructs (A) and blank scaffolds (B) after 2 wk of implantation, Masson's trichrome (C) staining of 2 wk implants of constructs (collagenous ECM stained blue). Immunohistochemical staining of IgG control 2 wk after implantation (D), the donor and host derived SMCs stained with SM-α-actin antibody (E) and the donor-derived HASMCs stained with human mitochondria antibody (F). Scale bar: 200μm.

Table 1

Primers used for qRT-PCR

Gene	Primer sequence	GeneID	Product size (bp)
18S RNA	forward: 5′-ggaagggcaccaccaggagt-3′ reverse: 5′-tgcagccccggacatctaag-3′	100008588	317
MyoCD	forward: 5′-ctgggacgacatggaaaa-3′ reverse: 5′-acatggctgggacattga-3′	93649	191
SMMHC	forward: 5′-agagacagcttcacgagtatgag-3′ reverse: 5′-cttccagctctctttgaaagtc-3′	4629	398
Smoothelin	forward: 5′-cctggatacagaggacatgg-3′ reverse: 5′-caggtggttgtagagcgact-3′	6525	157